Available online at www.sciencedirect.com
ScienceDirect

Journal of Magnetism and Magnetic Materials 310 (2007) 2038–2040

Journal of magnetism and magnetic materials

www.elsevier.com/locate/jmmm

Field- and current-driven domain wall dynamics: An experimental picture

G.S.D. Beach*, C. Knutson, M. Tsoi, J.L. Erskine

Department of Phyiscs, The University of Texas at Austin, Austin, TX 78712-0264, USA

Available online 28 November 2006

Abstract

Field- and current-driven domain wall velocities are measured and discussed in terms of existing spin-torque models. A reversal in the roles of adiabatic and non-adiabatic spin-torque is shown to arise in those models below and above Walker breakdown. The measured dependence of velocity on current is the same in both regimes, indicating both spin-torque components have similar magnitude. However, the models on which these conclusions are based have serious quantitative shortcomings in describing the observed field-driven wall dynamics, for which they were originally developed. Hence, the applicability of simple one-dimensional models to most experimental conditions may be limited.

PACS: 75.60.Ch; 85.75.-d; 75.75.+a

Keywords: Spin-transfer torque; Domain wall dynamics; Ferromagnetic nanowire

The capacity of a spin-polarized current to move a domain wall is experimentally well established [1–3], but the mechanisms responsible for that motion [4–9] remain under debate. Models fall into two classes, termed "adiabatic" [4–6] and "non-adiabatic" [5,7–9]. Most analytical work has cast these interactions within the framework of one-dimensional (1D) domain wall dynamics formulated decades ago [10]. Here we outline the predicted wall dynamics, present experimental characterizations of these dynamics, and discuss them in terms of the 1D models. Interpretation of the data within a 1D model framework provides estimates of relevant spin-torque parameters. However, the same model predicts key parameters of field-driven motion at odds with experiment by up to three orders of magnitude. The quantitative failure of the 1D model to describe field-driven motion warrants caution in directly extending the model to current-driven motion.

A wall geometry appropriate for most recent experiments [2,3] is shown in Fig. 1. The orientation of each spin is denoted (θ, ϕ), and θ(x) varies from 0 to π over a characteristic width Δ [10]. The wall is described by two collective coordinates derived from θ and ϕ: the wall displacement q and its canting angle ψ. Wall motion requires a torque on θ to bring the wall spins toward the applied field H_a. However, H_a applies a torque not to θ, but to ϕ, and thus cannot directly drive wall motion. Instead, $H_a$cants ψ away from the easy plane and a demagnetizing field $H_d$develops. It is the demagnetizing torque, $\gamma\vec{M} \times \vec{H}_d$, that drives θ and consequent wall motion $\dot{q}$. The existence of a velocity maximum [10] then follows naturally. At $\psi = \pi/4$, the demagnetizing torque, and thus $\dot{q}$, peaks. If H_a drives ψ past this limit, ψ can no longer remain

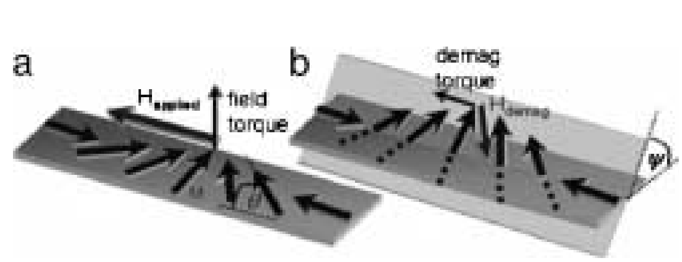

Fig. 1. Domain wall subjected to an axial field.

*Corresponding author. Tel.: +1 512 471 7073; fax: +1 512 471 6518.
E-mail address: gbeach@physics.utexas.edu (G.S.D. Beach).

0304-8853/$ - see front matter © 2006 Elsevier B.V. All rights reserved.
doi:10.1016/j.jmmm.2006.10.946

stationary, a transition termed Walker breakdown. ψ advances continually and the demagnetizing torque contribution to $\dot{q}$, $(\gamma\vec{M} \times \vec{H}_d)$, changes direction with each quarter period, averaging to zero. ψ rotation becomes more rapid with increasing H_a, leading to a small net damping torque $(\alpha\vec{M} \times \dot{\vec{M}})$ that cants the wall spins toward H_a and drives the wall forward. At high H_a, this damping torque provides the sole contribution to $\dot{q}$.

In this picture, the roles of adiabatic and non-adiabatic spin-torque are, loosely, to drive ψ and q motion, respectively, and the following equations of motion emerge [5,9]:

$$\dot{q} = (2\pi M_s)\gamma\, \Delta \sin 2\psi + \alpha\, \Delta\dot{\psi} + \eta u, \tag{1a}$$

$$\dot{\psi} = \gamma H_a - (\alpha/\Delta)\dot{q} + (\beta u)/\Delta. \tag{1b}$$

A current density j is included via $u = -(g\mu_B p/2eM_s)j$ [11]. β defines the strength of the non-adiabatic interaction, appearing in Eq. (1b), and is expected to be $\sim 10^{-2}$ [8,9]. Adiabatic torque appears in Eq. (1a), with $\eta \equiv 1$ in most models. There are two limiting cases, which occur below and far above breakdown: (I) $\dot{\psi} = 0$ and (II) $\dot{\psi} \gg 1$. The first represents stationary motion wherein $\dot{q}$ is dictated by Eq. (1b),

$$\dot{q}_I = (\gamma\Delta/\alpha)H_a + (\beta u)/\alpha. \tag{2}$$

Only the non-adiabatic term drives wall motion. ψ must adapt to maintain equality between Eqs. 1(a and b), andthe sole effect of adiabatic torque is to shift the steady-state ψ. Stationary motion exists only up to $\psi = \pi/4$, which occurs at

$$H_W = 2\pi\alpha M_s + (\alpha\eta - \beta)u/\gamma\Delta. \tag{3}$$

In case (II) the time-average $\langle \sin 2\psi \rangle \to 0$ in Eq. (1a). Neglecting terms of order α^2 and $\alpha\beta$ with respect to 1,

$$\dot{q}_{II} = \gamma\, \Delta\alpha H_a + \eta u. \tag{4}$$

In this precessional regime, adiabatic torque alone augments the wall velocity. Adiabatic and nonadiabatic interactions may thus be probed independently by using a field to select regime I or II via Eq. (3). To explore this, wall velocities v were measured in a $20\,nm \times 600\,nm$ $Ni_{80}Fe_{20}$ nanowire (Fig. 2), using high-bandwidth Kerr polarimetry [12]. The v–H curves of the left wall at $j = 0$ and $\pm 5.8 \times 10^{11}\,A/m^2$ are linear at low and high H, as expected from Eqs. (2) and (4), and exhibit a peak at $H_W = 6\,Oe$ marking breakdown. The zero-H data show an anomalous hump at intermediate H, which vanishes with j and whose cause is currently under investigation. Here we focus on low and high H, where j simply imparts a vertical shift to v(H). Although Eqs. (2) and (4) predict symmetric shifts about the $j = 0$ curve, the data show a positive current is more effective at increasing v than a negative current is at decreasing v.

To explore the symmetries of the interaction, v(j) was measured at various constant H, and the symmetric (v_+) and anti-symmetric (v_-) components, $v_\pm(j) = (v(+j) \pm v(-j))/2$, were determined. Results at $H = 44\,Oe$ are shown in Fig. 2. The data reveal a linear component in j with a nearly constant slope of $\sim 2.7 \times 10^{-7}\,m^3/C$ over the entire field range studied, and a nonlinear component that is quadratic at low and high H. We interpret the linear component within the model above, and find $\alpha/\beta \approx \eta \approx 1$. However, if the current characteristics are to be interpreted within this 1D model, then likewise must the field characteristics. Eqs. (2) and (4) predict the ratio of the slopes of v(H) above and below breakdown to be α^2, or $\sim 10^{-4}$, compared to a measured value ~ 0.15. Adiabatic torque is an analog of the precessional damping that drives wall motion well above breakdown and leads to the high-field mobility. Since the 1D model fails by a factor 10^3 to describe the latter, it is questionable how well it describes the former.

Likewise, Eq. (3) defines a breakdown field dependent on the perpendicular anisotropy and current. We find no more than a $\sim 10\%$ change in H_W over the current range studied, implying $\alpha/\beta \approx \eta$. However, Eq. (3) also predicts a zero-j

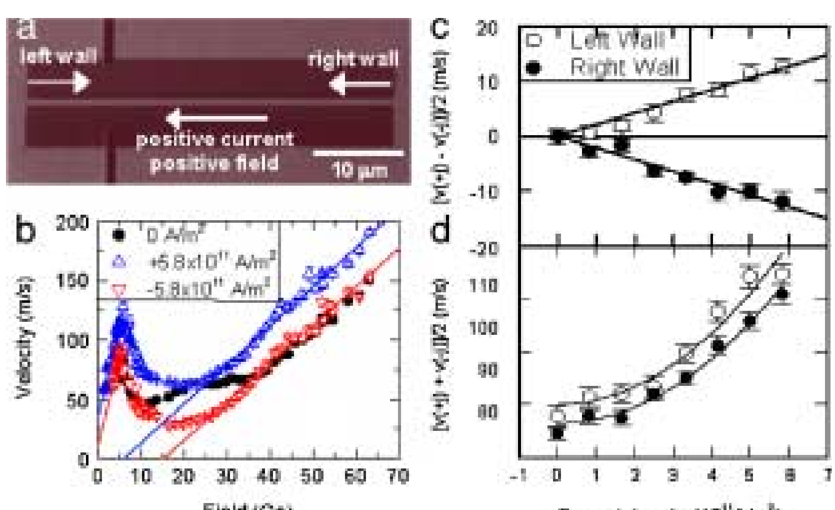

Fig. 2. (a) Plan-view SEM image of nanowire structure. For $j > 0$ e^- flow to the right, (b) mobility curves of left wall for three currents. (c) Odd and (d) even v(j) components at $H = 44$.

breakdown field of ~50 Oe, 10 times larger than the observed 6 Oe, at which the canting angle ψ is only ~4°. Since the non-adiabatic component is analogous to a field, if the model fails to describe field-driven breakdown by an order of magnitude, it is questionable that variations in H_W can be reliably used to gauge the magnitude of β.

The failure of the 1D model to describe field-driven motion implies that its direct application to current-driven motion may be of limited value. Indeed, no 1D model has predicted the observed nonlinear component in v(j), although its effect can exceed that of the linear component at moderate j. Meaningful comparison between experiment and theory will require models that fully account for realistic, time-variant domain structures, such as the vortex walls known to prevail in many experimental situations [13,14].

Work supported by the NSF-NIRT program (DMR-0404252) and the R.A. Welch Foundation (F-1015). Instrumentation developed through the NSF IMR program (DMR-0216726) and the Texas Co-ordinating Board (ATP-0099). Facilities were used at the Center for Nano and Molecular Science and Technology at UT Austin.

References

[1] P.P. Freitas, L. Berger, J. Appl. Phys. 57 (1985) 1266.
[2] M. Kläui, et al., Appl. Phys. Lett. 83 (2003) 105.
[3] M. Tsoi, et al., Appl. Phys. Lett. 83 (2003) 2617.
[4] L. Berger, J. Phys. Chem. Solids 35 (1974) 947.
[5] G. Tatara, H Kohno, Phys. Rev. Lett. 92 (2004) 086601.
[6] Z. Li, S. Zhang, Phys. Rev. Lett. 92 (2004) 207203.
[7] L. Berger, J. Appl. Phys. 55 (1984) 1954.
[8] S. Zhang, Z. Li, Phys. Rev. Lett. 93 (2004) 127204.
[9] A. Thiaville, et al., Europhys. Lett. 69 (2005) 990.
[10] A.P. Malozemoff, J.C. Slonczewski, Magnetic Domain Walls in Bubble Materials, Academic Press, New York, 1979.
[11] Polarization p taken as 0.4, and $M_s = 800$ emu/cc for $Ni_{80}Fe_{20}$.
[12] G.S.D. Beach, et al., Nat. Mater. 4 (2005) 741.
[13] R.D. McMichael, et al., IEEE Trans. Magn. 33 (1997) 4167.
[14] Y. Nakatani, et al., Nat. Mater. 2 (2003) 521.